Physica C 206 (1993) 360–366
North-Holland

PHYSICA C

Magnetooptic observation of the Meissner effect in $YBa_2Cu_2O_{7-x}$ single crystals

L.A. Dorosinskii, M.V. Indenbom, V.I. Nikitenko, A.A. Polyanskii, R.L. Prozorov and V.K. Vlasko-Vlasov

Institute of Solid State Physics, Russian Academy of Sciences, Chernogolovka, Moscow distr., 142432, Russian Federation

Received 30 November 1992

We report the first real-time, direct magnetooptic images of the Meissner effect in doped $YBa_2Cu_3O_{7-x}$ single crystals. Measurements of flux profiles across field-cooled samples reveal increased pinning due to impurities. The strongest effect of the present dopants (Mn, Ca or Si) was found for Si. Furthermore, the spatial resolution was sufficient to observe enhanced trapping of vortices in heavily twinned regions, indicating a strong contribution of twin boundaries to pinning at higher temperatures.

1. Introduction

Pinning centers providing high critical current densities over a wide temperature range are essential for the application of high-temperature superconductors. Spatial information on microstructural features involved in flux trapping can be obtained by direct observation of the mixed state structure. Real-time spatial information on flux trapping and expulsion would allow correlation to be established with microstructural details characterized by other means and thus reveal the most effective pinning mechanisms. In the present work, the expulsion of magnetic flux during cooling $YBa_2Cu_3O_{7-x}$ (YBCO) single crystals in a magnetic field (i.e., the Meissner effect) was studied using a new technique of imaging with magnetooptic garnet films possessing in-plane magnetic anisotropy [1]. The enhanced resolution and sensitivity of these films compared to the films with perpendicular magnetic anisotropy [2] provides new opportunities for correlating flux pinning with defect structures. Recently this technique was used for visualization of the Meissner expulsion of the magnetic field from undoped YBCO crystals [3]. Reported here are observations of the Meissner effect, flux trapping by twin boundaries, and effects of various dopants on the Meissner effect in YBCO single crystals.

2. Experimental techniques

Single crystals of YBCO for this study were grown by a flux method described previously [4]. Crystals grown by this method contain approximately 1 at.% Au, situated exclusively on the Cu(1) site [5]. In addition to Au impurities, some crystals were intentionally doped with either Ca, Mn, or Si by adding the appropriate dopant oxide to the initial charge for crystal growth. Dopant concentrations were determined by energy dispersive X-ray spectrometry. For simplicity, crystals containing only Au impurities will be referred to in this paper as "undoped".

Individual crystals were rectangular prisms, typically 100–300 μm in the a/b direction by 50–150 μm in the c direction. Crystals were examined using reflected polarized light to ascertain twin structures. Twin domains in most crystals were very small, typically <1 μm. Some samples exhibited fairly large untwinned areas, up to several tens of micrometers wide, most frequently in the corners of the crystals.

The superconducting onset temperature (T_c) was measured from macroscopic susceptibility curves in a weak AC field. The onset temperature was ~90 K

with a transition width of ~2 K for all crystals except the Ca-doped samples. The Ca-doped crystals showed a transition temperature of 75 K with a width of ~4 K. Crystal dimensions, dopant concentrations, T_c and ΔT_c values for all crystals and also fractions of the Meissner flux expulsion are given in table 1.

The magnetic flux distribution was imaged using thin iron-garnet indicator films with in-plane anisotropy [1]. Samples were placed on the cold finger of a helium microcryostat using a thin layer of adhesive to ensure good thermal contact. The broad (001) surface of a crystal was covered with the indicator film and induction in the film could be analyzed in polarized light due to the Faraday effect. A DC magnetic field was applied normal to the surface under study, i.e., along the *c*-axis of the crystal. In such a geometry the indicator film allows the measurement to be made of the normal component of induction in the sample which results in a magnetization declination out of the film plane and thus in an increase of the magnetooptic image intensity.

Images were recorded on video tape and compared with the twin structure of the crystals. In addition magnetic flux profiles along selected directions in the samples were measured by photometry as described in ref. [1]. Scanning was accomplished by a computer controlled step motor. The diameter of the photometering diaphragm corresponded to a 4 μm circle in the sample plane. Changes in the Meissner fraction with temperature in different sample regions were measured using a photometered area ~40 μm in diameter.

3. Results and discussion

Meissner expulsion of the magnetic flux was observed during cooling a crystal below T_c in a DC magnetic field applied perpendicular to the surface of the sample. Above T_c the superconductor exhibited no screening effect and the entire indicator film was monotonically colored. However, below T_c screening currents caused partial expulsion of the flux from a crystal, resulting in an inhomogeneous image wherein regions of higher flux density (brighter areas) and lower flux density (darker areas) were revealed (e.g. see fig. 1). The largest exit of flux occurred near the crystal edges as indicated by the dark stripe along the perimeter of the sample. In addition, differences in the Meissner fraction were readily observed in the central region of the (001) face, suggesting differences in defect structures. The degree of flux expulsion increased with decreasing temperature; at ~10 K below T_c the image was stabilized and did not change with further reduction in temperature, indicating vortex freezing at the pinning centers.

More detailed features of the magnetic flux distribution in field-cooled samples are visible in the induction profiles which were measured along selected directions in the crystals. Figure 2 shows typical examples of Meissner profiles for an undoped crystal at 40 K for two different values of the field [3]. Near the crystal edges there is a drop in the magnetic induction resulting from flux expulsion whereas in the central area the higher induction values indicate that the vortices have been pinned. The shape of the induction profile near the crystal edges does not change significantly with increasing field.

This profile is consistent with the Meissner state

Table 1

Sample [a]	Dimension (μm)	Dopant concentration (ppm by weight)	T_c (onset) (K)	Transition width, ΔT (K)	Meissner fraction %			
					25 Oe		50 Oe	
					Untwinned	Twinned	Untwinned	Twinned
K–2	458×258×88	undoped	90	1.5	90	12	70	10
K–7	470×228×120	undoped	90	1.5	81	58	42	13
K(Mn)–3	246×180×65	1000	89	1.5	20	2	19	1
K(Ca)–3	143×226×72	6000	75	4.0	–	6	–	2
K(Si)–2	734×936×101	1500	87	2.5	–	<1	–	<1

[a] Crystals K(Ca)–3 and K(Si)–2 are densely twinned whereas K–2, K–7 and K(Mn)–3 contain areas with different twin density.

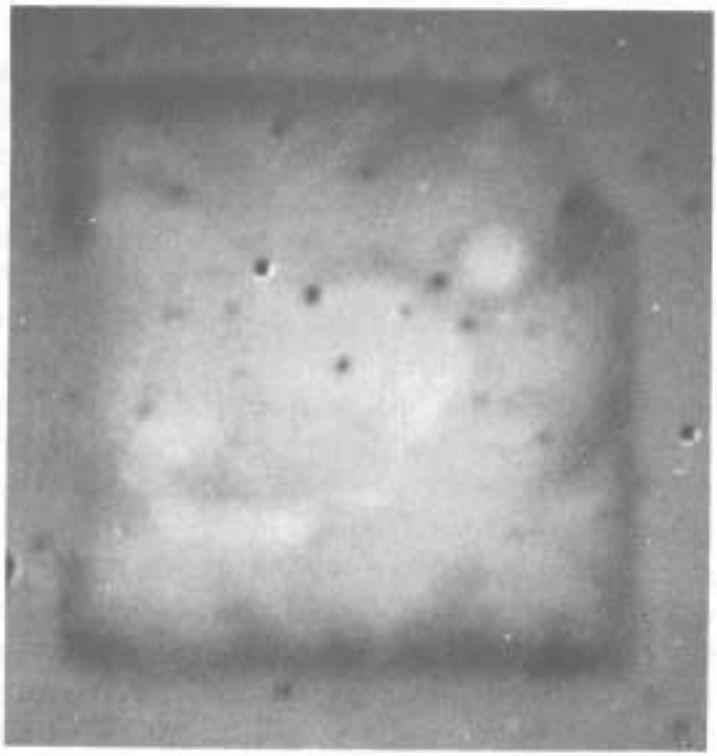

Fig. 1. Magnetooptical image showing the flux distribution in a field-cooled Y8CO undoped single crystal. The intensity of the image reflects the intensity of the component of the magnetic field normal to the indicator film. Flux expulsion near the crystal edges is clearly visible (dark area). $H_a = 100$ Oe, $T = 60$ K.

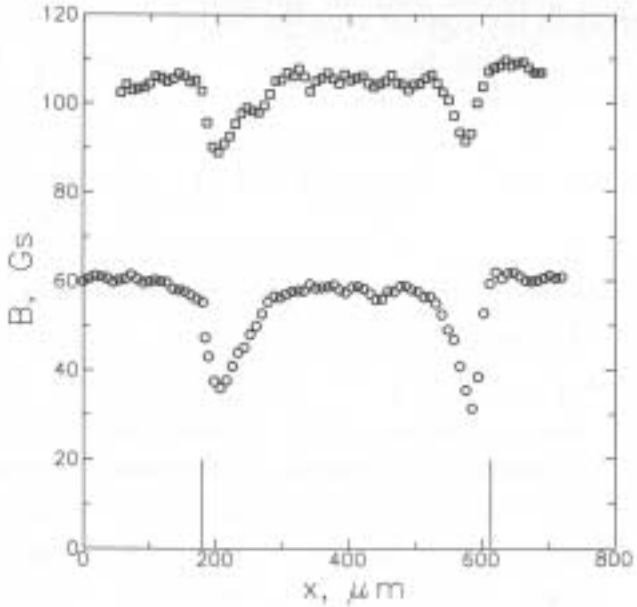

Fig. 2. Induction profiles measured across the undoped crystal at 40 K for $H_a = 107$ Oe and 60 Oe. Vertical lines on this figure and figs. 3, 4 and 6(a) show the sample edges.

model for hard type-II superconductors that was proposed by Moshchalkov et al. [6] and developed by Krusin-Elbaum et. al. [7]. In accordance with this model, the shape of the induction spatial distribution $B(x)$ is weakly dependent on the applied (external) field value H_a and changes rapidly only in the thin surface layer, producing a step in $B(x)$ which is proportional to the lower critical field $H_{c1}(T)$ for $H_{c1}(T) < H_a$.

At the same time, the external field sets a constant background on which these changes in $B(x)$ occur. The model proposes that the flux distribution within a crystal stops changing with decreasing temperature when $H_{c1}(T)$ becomes equal to H_a. Then, the step in induction at the surface is determined by the value mH_{c1}, as given by the equilibrial induction curve $B(H) \sim H_a - mH_{c1}$. The coefficient m is equal to one in the "triangular approximation" [6] and is taken to be less than one in ref. [7]. The latter value seems more appropriate as it corresponds to a steep increase of the equilibrial $B(H)$ curve at H_{c1}.

The region near the sample edge where after the surface step of induction the fastest flux density increase (approximately linear in distance from the edge) takes place has a width

$$L(T_{c1}) = \frac{mH_a c}{4\pi n J_c(T_{c1})} .$$

Here c is the velocity of light, T_{c1} is the temperature at which $H_{c1}(T) = H_a$, $J_c(T_{c1})$ is the critical current density which is suggested [6] to change with temperature as $J_c = J_{c0}(1 - T^2/T_c^2)^n$, and $H_{c1}(T) = H_{c10}(1 - T^2/T_c^2)$, where $H_{c10} = H_{c1}(T = 0)$. Taking $m \approx 0.5$, $H_a \approx 100$ Oe, $J_c(T_{c1}) \approx 10^5$ A/cm^2 and $n = 3$ gives $L(T_{c1}) \approx 1$ μm. Thus, as this distance is not resolved (because the measuring diaphragm has a diameter of 4 μm), the shape of the measured Meissner profiles should not change and they should only shift upwards with increasing field. These trends were observed in the profiles shown in fig. 2.

It should be noted that the above model does not take into account demagnetization effects that will modify the shape of the induction profile in the case of a plate subjected to a field normal to its large face [8,9]. Nevertheless, qualitative features of the flux profiles can be understood from the model results

[6,7]. The spatial distribution of induction has the form [7]

$$B(x)=H_a-\frac{(n-1)m}{n}H_{c10}\frac{(mH_{c10})^{1/(n-1)}}{x4\pi nJ_{c0}}.$$

This equation indicates that, when moving away from the crystal edge, the induction should rise rapidly from the minimum value H_a-mH_{c1} to some maximum value at the center of the sample. According to the above formula, the maximum value should decrease with decreasing critical current density. Thus, the lower the J_c value, the lower will be the induction in the center of the sample with respect to the external field value. Such behavior corresponds to the stronger flux trapping (higher induction) in the case of higher J_c values and to more pronounced flux expulsion (lower induction) for lower J_c values. Comparison of the flux profiles obtained in undoped (fig. 2) and doped YBCO crystals (e.g. figs. 3 and 4) clearly shows that flux expulsion in the doped crystals is much less than in the undoped ones. Thus, doping appears in increasing pinning or in higher critical current density. The strongest effect is observed in Si-doped crystals. It seems that the small size of the Si ion compared to the host ions could result in formation of point defects of an interstitial type producing strong internal stresses which are responsible for increasing pinning of the vortex lines.

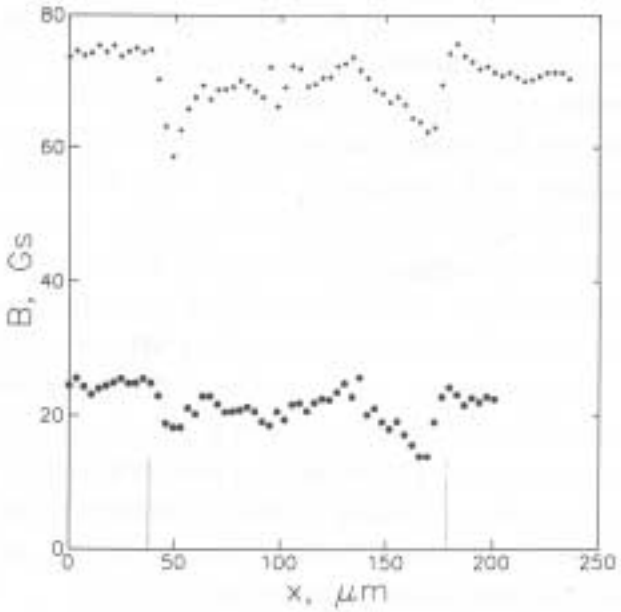

Fig. 3. Induction profiles in the Ca-doped crystal KCa-3 at 40 K for $H_a=75$ Oe and 25 Oe.

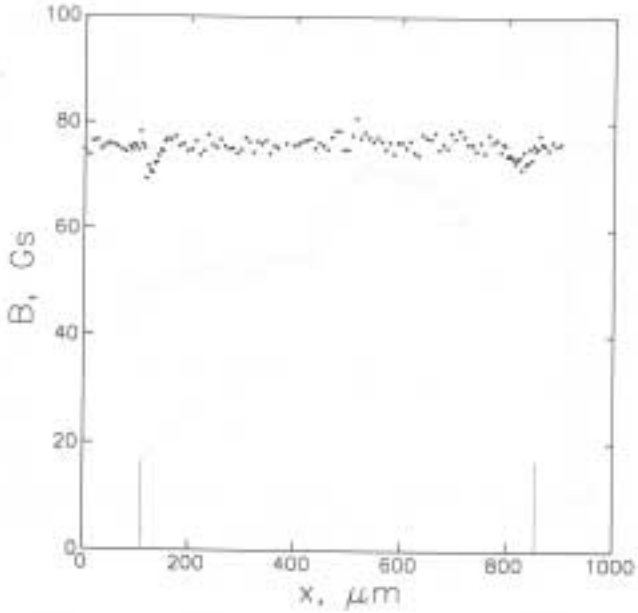

Fig. 4. Induction profile in the Si-doped crystal KSi-2 at 50 K and 75 Oe.

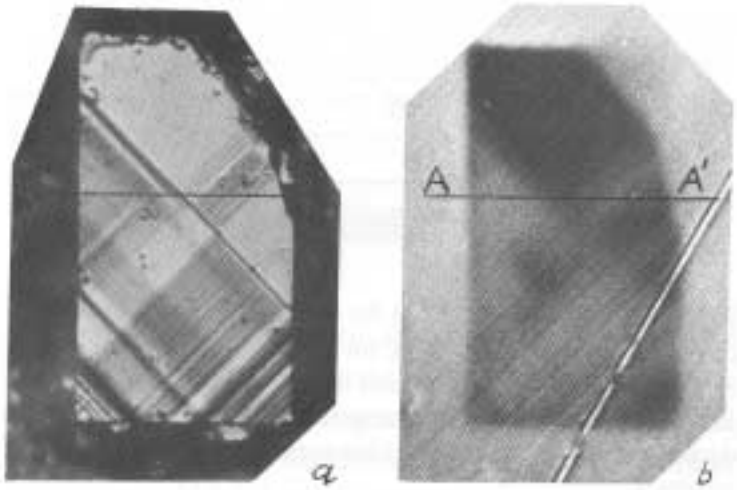

Fig. 5. (a) Twin structure in the undoped crystal K2 (untwinned areas are bright). (b) Magnetooptical image showing the effect of twins on flux expulsion during field-cooling $H_a=75$ Oe, $T=20$ K. Dark regions indicate a lower flux density as observed in the untwinned area.

Large differences in magnetic flux trapping in field-cooled samples were found for crystalline regions having different twin densities (fig. 5(a)). As seen in fig. 5(b), vortices escape more easily from the untwinned region and the sample corners having wide domains than from more finely twinned areas. The flux profile in fig. 6(a) measured along the line A–A′ indicated in fig. 5(b) confirms that the induction and, hence, the critical current density in the un-

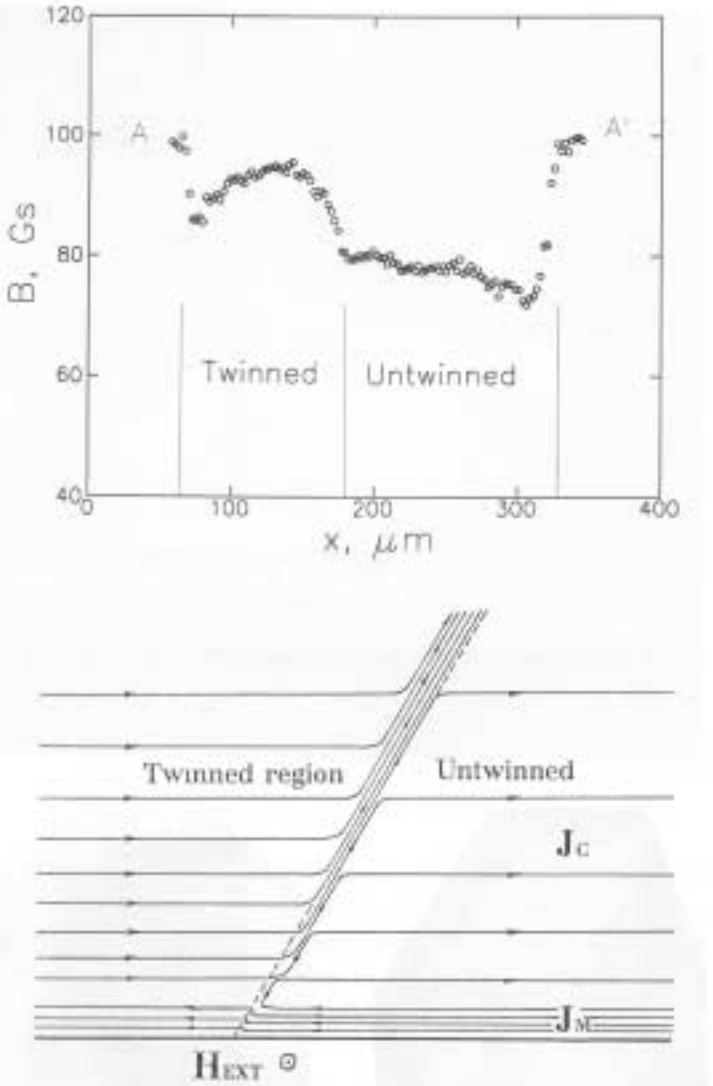

Fig. 6. (a) Induction profile in the undoped crystal K2 along the line A–A' (fig. 5(b)) at 20 K for $H_a = 100$ Oe. (b) Schematic representation of the distribution of the Meissner (J_M) and critical (J_c) currents in an inhomogeneously twinned crystal. The dashed line shows the boundary between twinned and untwinned regions.

twinned main region are substantially less than in the finely twinned area. This behavior is found evidence for by a decrease in the slope of $B(x)$ and a lower induction level in the untwinned region compared to the finely twinned region. In the untwinned region there are several narrow parallel twins crossing the scanning line, but their effect on the induction profile near the crystal edge and at the boundary between twinned and untwinned regions is insignificant.

From fig. 6(a) the conclusion can also be drawn that the superconducting currents flow not only along the crystal edges, but also along the boundary between the untwinned and twinned regions. The drop in induction near the crystal edge is larger in the untwinned than in the twinned area, indicating that the Meissner current J_m is larger in the untwinned region. However, the volume critical current density J_c is larger for the twinned area. Due to continuity of current trajectories, both current components must decline inside the crystal and create a current path along the boundary between the twinned and untwinned regions (fig. 6(b)). This behavior would result in a drop in induction at the boundary which is revealed in fig. 6(a). Thus the presence of twins not only increases pinning, but can also result in the redistribution of superconducting currents in the crystal. Since this large effect of twins on flux trapping in the Meissner experiment was observed at temperatures within ~10 K of T_c, twin boundaries may be effective pinning centers at higher temperatures. At lower temperatures, other defects may be more effective pinning centers, thereby overshadowing the contribution of twins so that the effect of twin boundaries on pinning is not revealed (see e.g. refs. [10–12]).

Macroscopic magnetization measurements (see e.g. ref. [6]) have shown that the Meissner fraction decreases strongly with increasing field. To study this effect, the average induction in 40 μm regions near the crystal edges was monitored as a function of temperature at different field values. Typical induction curves for the untwinned region of the undoped crystal K2 are shown in fig. 7. Flux expulsion is mostly complete by ~10 K below T_c. The amount of expelled flux (defined as $B_{ht} - B_{lt}$, where B_{ht} and B_{lt} are the induction values at the high and low temperature plateaus, respectively) changes only slightly with H_a. Thus, the Meissner fraction given by $(B_{ht} - B_{lt})/B_{ht}$ decreases with increasing field. The field dependences of the Meissner fraction (MF) in the untwinned and twinned regions of the same crystal are shown in fig. 8. The data of fig. 8 are satisfactorily described by the exponential curves MF ~ $(\exp - H_a/H^*)$ in accordance with results of the macroscopic susceptibility measurements in a twin-free TmBCO crystal cooled in a field applied along the c-axis [6]. Our experimental value of the constant H^*, defined from the computer fit of the data is 340 Oe, which is close to the value obtained in ref. [6].

However, in some crystals the dependence was not exponential. Figure 9 shows the Meissner fraction measured in twinned and untwinned areas of the un-

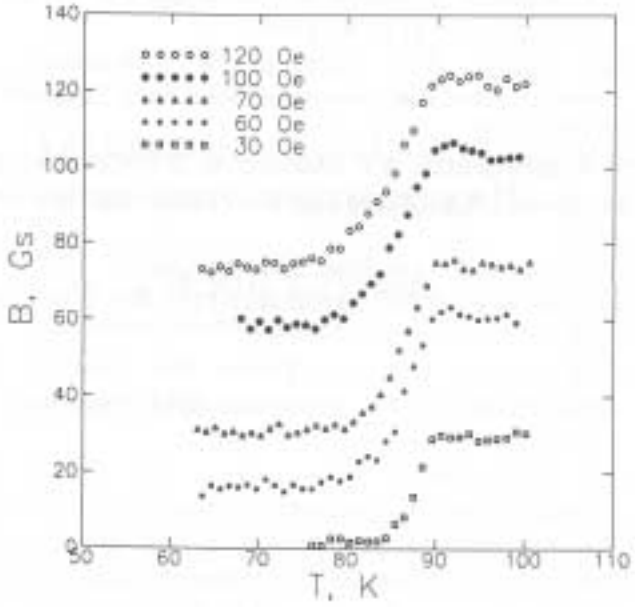

Fig. 7. Temperature dependence of induction in the undoped crystal K2 (in the untwinned region) at different fields. The magnetooptic signal was measured using a 40 μm diaphragm.

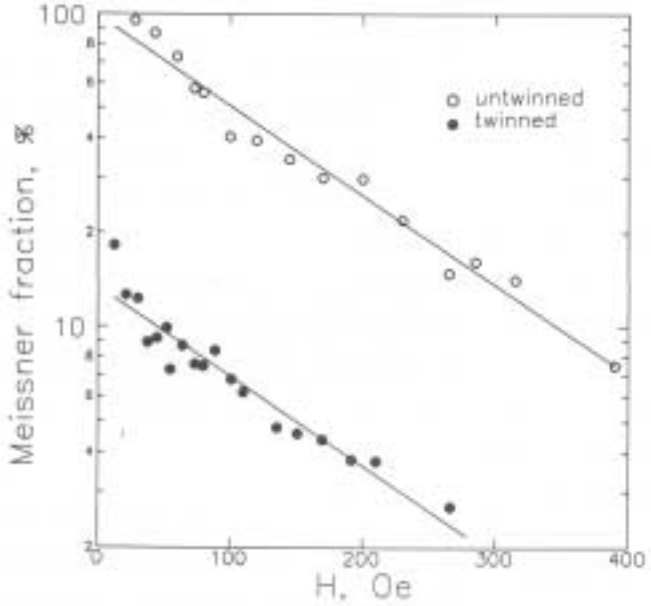

Fig. 8. Field dependence of the Meissner fraction in the untwinned and twinned regions in the undoped crystal K2. The Meissner fraction is estimated from curves similar to those shown in fig. 8 as the difference between induction at the high and low temperature plateaus.

doped crystal K7. The data of fig. 9 do not follow the exponential behavior but fit better to $MF \sim 1/H_a^{\alpha}$, where $\alpha \approx 0.8$ for twinned and $\alpha \approx 0.2$ for untwinned regions. This corresponds to $n=2.8$ (twinned) and $n=2.2$ (untwinned) for the temperature dependence of the critical current density $J_c \sim (1-T^2/T_c^2)^n$ in ref. [7]. Thus the stronger decrease of

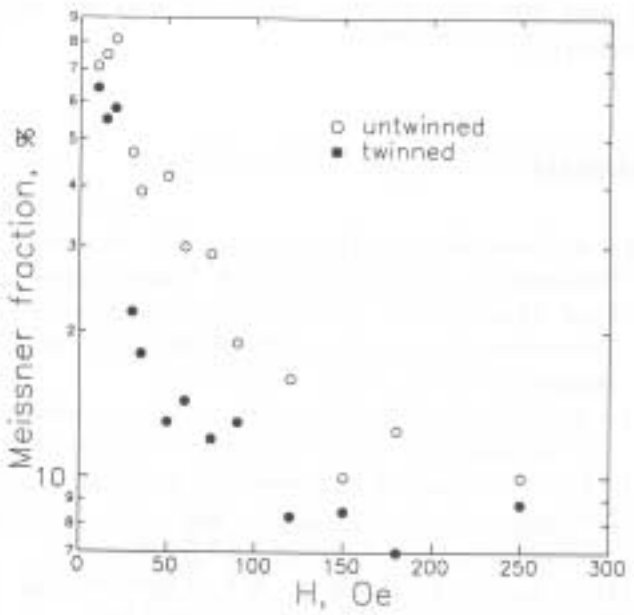

Fig. 9. Field dependence of the Meissner fraction for the finely twinned and monodomain areas in the undoped crystal K7.

the Meissner fraction in the finely twinned area as compared to the untwinned region can be associated with a more rapid drop of the critical current density with temperature in the twinned than in the untwinned area.

4. Conclusions

Direct observations of the flux distributions in field-cooled YBCO crystals have been made for the first time using a recently improved magnetooptical imaging technique. Distributions of magnetic flux in the present YBCO single crystals correspond qualitatively to a recent model of vortex trapping in hard type-II superconductors [6,7]. It has also been shown that doping with Ca, Mn and Si decreases the Meissner fraction and enhances flux pinning and trapping in crystals.

Measurement of crystals with inhomogeneous twin densities revealed that the fraction of expelled flux is significantly lower in regions of high twin density compared to untwinned regions. This result suggests that twin boundaries play a significant role in vortex pinning in YBCO at higher temperatures.

Acknowledgement

The authors thank D. Kaiser for the YBCO crys-

tals and for the improvement of English of the manuscript.

References

[1] A.A. Polyanskii, L.A.Dorosinskii, M.V. Indenbom, V.I. Nikitenko, Yu.A. Ossip'yan and V.K. Vlasko-Vlasov, in: Int. Conf. Advanced Materials - ICAM 91, Symposium A1: High Temperature Superconductor Thin Films (27–31 May 1991, Strasbourg, France), Proc. v. 14, p. 1300.

[2] A.A. Polyanskii, V.K. Vlasko-Vlasov, M.V. Indenbom and V.I. Nikitenko, Sov. Tech. Phys. Lett. 15 (1989) 872.

[3] V.K. Vlasko-Vlasov, L.A. Dorosinskii, M.V. Indenbom, V.I. Nikitenko, A.A. Polyanskii and R.L. Prozorov, Sverkhprovodimost' 5 (1992) 2017 (in Russian).

[4] D.L. Kaiser, F. Hotzberg, M.F. Chisholm and T.K. Worthington, J. Cryst. Growth 85 (1987) 593.

[5] D.L. Kaiser, F. Hotzberg, B.A. Scott and T.R. Mc Guire, Appl. Phys. Lett. 51 (1987) 1040.

[6] A.A. Zhukov, V.D. Kuznetsov, V.V. Metlushko, V.I. Voronkova and B.K. Yanovskii, Solid State Commun. 74 (1990) 1295.

[7] L. Krusin-Elbaum, A.P. Malozemoff, D.C. Cronmeyer, F. Hotzberg, J.R. Clem and Zh. Hao, J. Appl. Phys. 67 (1990) 4670.

[8] D.J. Frenkel, J. Appl. Phys. 50 (1979) 5402.

[9] M. Daumling and D.C. Larbalestier, Phys. Rev. B 40 (1989) 9350.

[10] E.M. Gyrogy, R.B. van Dover, K.A. Jackson, L.F. Schneemeyer and J.V. Waszczak, Appl. Phys. Lett. 55 (1989) 283.

[11] V.V. Moshchalkov, A.A. Zhukov, D.K. Petrov, V.I. Voronkova and V.K. Ynaovskii, Physica C 166 (1990) 185.

[12] V.K. Vlasko-Vlasov, L.A. Dorosinskii, M.V. Indenbom, V.I. Nikitenko, A.A. Polyanskii, A.V. Antonov, Yu.M. Gusev and G.A. Emel'chenko, Supercond. 4 (1991) 1007.